New Advances in Stellar Physics: From Microscopic to Macroscopic Processes
G. Alecian, Y. Lebreton, O. Richard and G. Vauclair (eds)
EAS Publications Series, **63** *(2013) 321–330*

IPOPv2: PHOTOIONIZATION OF Ni XIV – A TEST CASE

F. Delahaye[1], P. Palmeri[2], P. Quinet[2,3] and C.J. Zeippen[1]

Abstract. Several years ago, M. Asplund and coauthors (2004) proposed a revision of the Solar composition. The use of this new prescription for Solar abundances in standard stellar models generated a strong disagreement between the predictions and the observations of Solar observables. Many claimed that the Standard Solar Model (SSM) was faulty, and more specifically the opacities used in such models. As a result, activities around the stellar opacities were boosted. New experiments (J. Bailey at Sandia on Z-Pinch, The OPAC consortium at LULI200) to measure directly absorbtion coefficients have been realized or are underway. Several theoretical groups (CEA-OPAS, Los Alamos Nat. Lab., CEA-SCORCG, The Opacity Project – The Iron Project (IPOPv2)) have started new sets of calculations using different approaches and codes. While the new results seem to confirm the good quality of the opacities used in SSM, it remains important to improve and complement the data currently available. We present recent results in the case of the photoionization cross sections for Ni XIV (Ni^{13+}) from IPOPv2 and possible implications on stellar modelling.

1 Introduction

Recent studies on the solar abundances of elements have questioned the accuracy of the available sets of opacities. Asplund *et al.* (2004) proposed an abundance for oxygen which was much reduced as compared to previous values. Decreased values for the C and N abundances were also recommended. One of the consequences was to upset seismology findings so far considered reliable (depth of the convection zone, He content at the surface, sound speed profile) and one suggested way out of this difficulty was to modify the stellar opacities. Even though the revisited abundances have increased again since 2004, the debate is going on about the

[1] LERMA, Observatoire de Paris, ENS, UPMC, UCP, CNRS, 5 place Jules Janssen, 92195 Meudon Cedex, France
[2] Astrophysique et Spectroscopie, Université de Mons – UMONS, 7000 Mons, Belgium
[3] IPNAS, Université de Liège, 4000 Liège, Belgium

DOI: 10.1051/eas/1363036

reliability of the opacities used by the astrophysical community and about the relevance of the "new solar abundances" (see for example Pinsonneault & Delahaye 2009; Delahaye *et al.* 2010; Nahar *et al.* 2011; Delahaye & Pinsonneault 2006, DP06 hereafer).

This debate ignited several efforts to quantify the uncertainties on the opacities. Experimental work is under way using powerful lasers at LULI2000 (Gilles *et al.* 2011) or Z-pinch machine (Bailey *et al.* 2009) in order to measure opacities. Dedicated theoretical work and systematic comparisons between different findings for conditions characterizing the solar structure have been started within the OPAC consortium. Some results and comparisons for Fe and Ni are already available (see for example Turck-Chièze *et al.* 2012).

As presented in Badnell *et al.* (2005) or DP06, the mean opacities from the OP for mixtures like the solar case agree well with other work like OPAL (Rogers & Iglesias 1992) and LEDCOP (Magee *et al.* 1995). More recent calculations from the OPAS group (Blancard *et al.* 2012, B12 hereafter) also agree very well. Also, it is worth mentioning that modeled helioseismic tests have been performed with LEDCOP opacities (Neuforge-Verheecke *et al.* 2001) as well as with OPAL and OP data (DP06), showing good agreement in the prediction of solar observables. This gives us a pretty good confidence in the quality of the Rosseland mean opacities provided for solar models. However, as shown in Bailey *et al.* (2007), the details of the monochromatic opacities for certain elements may show sizeable differences with experimental data. Delahaye and Pinsonneault (2005) and The OPAS group (B12) also provided detailed comparisons for individual elements showing large differences. While these differences will not affect our results on the solar abundances presented in DP06, it is essential to quantify and understand them. The effect of remaining discrepancies could be of more consequence when running an evolutionary code. Discrepancies on spectral opacities for individual elements will modify the velocity of microdiffusion processes which in turn will influence the structure and evolution of intermediate mass stars (Richard *et al.* 2001; Delahaye & Pinsonneault 2005). It also will impact the condition of pulsating stars as shown in Montalban and Miglio (2008).

The present work present partial results for the Ni atomic data. The goal is to evaluate the two different approaches (R-matrix and independent-processes, isolated-resonance, distorted-wave (IPIRDW)) to calculate photoionization cross sections for the Ni XIV ion and estimate the impact on the opacities. In the next section we present the strategy and highlight the main differences on two approaches used to calculate the cross sections. In Section 3 we describe the calculations of cross sections in both methods. In Section 4 the results are presented comparing the different approaches and estimate the consequences on the opacities. We present the conclusion and perspective in the last section.

2 Strategy

Opacities are a property of a medium characterizing its resistance to the transfer of light. In the dertermination of such absorption coefficients, one has to take into

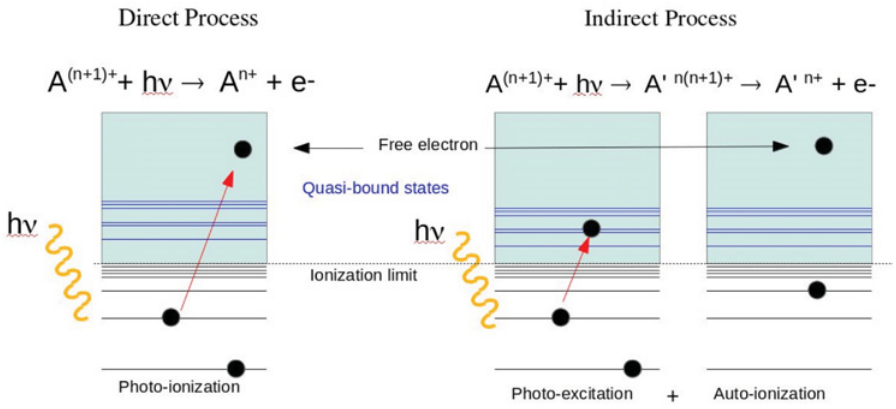

Fig. 1. Photoionization: 1 or 2 steps processes.

account different processes, photo-excitation, scattering and photoionization . For each element at each frequency point, the combination of these processes gives the total contribution of the element (see Eq. (2.1))

$$\kappa_{tot}(\nu) = \kappa_{bound-bound}(\nu) + \kappa_{bound-free}(\nu) + \kappa_{free-free}(\nu). \tag{2.1}$$

In order to derive the Rosseland mean, we have to sum up these contributions. Depending on the element and the physical conditions, the contribution of each processe will vary. In the case of stellar interiors and specificaly in the case of the sun, for all metals, the contribution from the photionization is dominant as shown in B12. In our project to quantify all uncertainties in the process of calculating opacities, it is then a good starting point to look at the photoionization cross sections. In the present work we look at the effect of the different methods to calculate the photoionization absorption cross section and the impact on the derived opacities.

For the conditions we are interested in, they are two main ways to photoionize an atom. There is the direct process where one photon is absorbed and takes one electron away from the atom to make it free (see Eq. (2.2)) and there is the indirect path where the photon excites one electron into an autoionizing state (also called quasi bound state) which autoionizes faster than it decays radiatively (see Eq. (2.3)). This is illustrated in Figure 1.

Direct process:

$$A_i^{N+1} + h\nu \rightarrow A_f^N + e^-. \tag{2.2}$$

Indirect process (also called photoexcitation-autoionization):

$$A_i^{N+1} + h\nu \rightarrow A_j^{N+1} \rightarrow A_f^N + e^-, \tag{2.3}$$

Both processes can interfere and give rise to resonances that display Beutler-Fano profiles (Fano 1961) in the cross sections.

The quality of OP opacities, especialy when looking at monochomatic opacity details for certain elements (Fe, Ni) (Bailey *et al.* 2009; Nahar *et al.* 2011; Turck-Chièze *et al.* 2012), can legitimately be questionned, even if it has been shown that the Rosseland mean opacities of a solar mixture are in very good agreement (DP06, B12). Moreover, the spectral opacities provided by OP include Mn, Cr and Ni. However the atomic data for these elements are not available. Their spectral opacities have been determined using Fe atomic data via a scaling procedure.

The goal of the present work is to estimate the impact of the different approximations and different methods on the atomic data and on the spectral opacities in detail. We want to quantify the uncertainties due to such choices (R-matrix *vs.* IPIRDW, direct calculations *vs.* scaling, LS coupling vs intermediate coupling) on opacities and estimate the impact on application after propagation of these uncertainties.

More specifically, in the present work, depending on the methods used to calculate the corresponding cross sections, the treatment of resonances will be drastically different. In the R-matrix method, both path for photoionization are included naturaly and are interfering, giving rise to Beutler-Fano resonances. In the IPIRDW method on the other hand, the inteference phenomena is neglected. Only lines appear on top of the continuum. A priori it would be more appealing to choose the more complete methods and be more accurate. However in calcuating opacities it is always a question of balance between completeness and accuracy. R-matrix calculations are far more demanding in order to include a large enough target and do not allow any treament of the broadening of the lines (resonances) while IPIRDW calculations allow to extend at will the number of lines included to take into account the resonances and it is possible to apply a profile for the broadening.

3 Photoionization cross section calculations

3.1 R-matrix method

One set of photoionization cross sections in this work has been calculated using the Breit-Pauli R-matrix method (*e.g.* Berrington *et al.* 1995) as employed in the Iron Project (IP) and utilized in a number of previous publications. The aims and methods of the IP are presented in Hummer *et al.* (1993). We briefly summarize the main features of the method and calculations. In the close coupling (CC) approximation the wavefunction expansion, $\Psi(E)$, for a total spin and angular symmetry $SL\pi$ or $J\pi$, of the (N + 1) electron system is represented in terms of the target ion states as

$$\Psi(E) = A \sum_i \chi_i \Theta_i + \sum_j c_j \Phi_j$$

where χ_i is the target ion wavefunction in a specific state $S_i L_i \pi_i$ or level $J_i \pi_i$, and Θ_i is the wavefunction for the (N + 1)th electron in a channel labelled as $S_i L_i (J_i) \pi_i i k_i^2 l_i (SL\pi)[J\pi]$; k_i^2 is the incident kinetic energy. In the second sum

the Φ_j are correlation wavefunctions of the (N + 1) electron system that (a) compensate for the orthogonality conditions between the continuum and the bound orbitals, and (b) represent additional short-range correlations that are often of crucial importance in scattering and radiative CC calculations for each symmetry. The Φ_j are also referred to as bound channels, as opposed to the continuum or free channels in the first sum over the target states. In the Breit-Pauli R-matrix calculations the set of $SL\pi$ are recoupled in an intermediate (pair) coupling scheme to obtain (e + ion) states with total $J\pi$, followed by diagonalization of the (N + 1)-electron Hamiltonian.

In the present work the target expansion for the CC calculations consists of 23 LS terms with principal quantum number up to $n = 4$ giving rise to 812 levels. The target eigenfunctions were developed using the AUTOSTRUCTURE program (Badnell 2011) an extension of SUPERSTRUCTURE (Eissner *et al.* 1974; Nussbaumer & Storey 1978).

The full expansion is $3s^23p^2+3s3p^3+3s^23p3d+3s3p^23d+3p^4+3p^33d+3s^23d+3p^23d^2+3s3p3d^2+3p3d^3+3s3d^3+3s^23p4l$ $(l = 0-3)+3s3p^24l(l = 0-3)+3p^34l$ $(l = 0-3)$. with the scaling factors, $\lambda_{1s} = 1.40434, \lambda_{2s} = 1.12157, \lambda_{2p} = 1.06304, \lambda_{3s} = 1.13180, \lambda_{3p} = 1.09963, \lambda_{3d} = 1.12434, \lambda_{4s} = 1.15189, \lambda_{4p} = 1.11693, \lambda_{4d} = 1.14682, \lambda_{4f} = 1.29663$ in the Thomas-Fermi-Dirac-Amaldi (TFDA) potential, $V(\lambda_{nl})$, employed in AUTOSTRUCTURE. This target is used in both methods (R-matrix and IPIRDW) in order to minimise the differences between the two runs in order to determine precisely the effect of each ingredient, in this case the configuration interaction on the resonance part of the cross sections.

In order to estimate the quality of the target wavefunction expansion, we compare the energy levels and the transition probabilities with those from the National Institute for Standards and Technology (Kramida *et al.* 2013; Shirai *et al.* 2000; Fuhr *et al.* 1988). The errors are of the order of 3.8% maximum for the energy levels and within 15% for all lines but one for which the error reach 30%. However it is difficult to rate the level of agreement since the stated NIST accuracy is no better than 50% for these transitions.

3.2 IPIRDW method

The photoionization cross sections of all the bound states of Ni^{13+} up to $nl = 10g$ have been computed using the atomic structure code AUTOSTRUCTURE. It computes term energies and/or fine-structure level energies, radiative and Auger rates, photoionization cross sections and electron-impact collision strengths. In these calculations, the atomic orbitals are constructed by diagonalizing the non-relativistic Hamiltonian within a scaled statistical TFDA model potential. The scaling parameters are optimized variationnally by minimizing a weighted sum of the LS term energies. LS terms are represented by configuration-interaction (CI) wavefunctions of the type

$$\Psi(LS) = \sum_i c_i \, \Phi_i. \tag{3.1}$$

Continuum wavefunctions are constructed within the distorted-wave (DW) approximation. Relativistic fine-structure levels and rates can be obtained by diagonalizing the Breit-Pauli Hamiltonian in intermediate coupling. The one- and two-body operators − fine-structure and non-fine structure − have been fully implemented to order $\alpha^2 Z^4$ where α is the fine-structure constant and Z the atomic number.

The non-resonant direct photoionization process (DPI, Eq. (2.2)) has been treated separately from the photoexcitation-autoionization (PAI, Eq. (2.3)) process within the framework of the IPIRDW approximation (Badnell & Seaton 2003; Fu *et al.* 2008).

In order to compare with our R-matrix calculation, we have computed the cross sections in LS coupling and used the same interacting configurations to describe the target of the scattering problem. The scaling parameters for the target orbitals, *i.e.* 1s to 4f, were identical to our R-matrix model. Relativistic corrections have been included in the orbital calculations by adding to the radial equations the mass-velocity and the Darwin terms.

Separate calculations have been performed for each initial complex of Ni^{13+}. For the $n = 3, 4$ complex we have considered the following DPI and PAI channels

$$\{3l^4, 3l^3 4l\}\{3l, 4l\} + h\nu \rightarrow \{3l^4, 3l^3 4l\} + e^-(kl'') \tag{3.2}$$

$$\begin{aligned} \{3l^4, 3l^3 4l\}\{3l, 4l\} + h\nu &\rightarrow \{3l^4, 3l^3 4l\}n'l'(n' > 4, l' \leq 5) \\ &\rightarrow \{3l^4, 3l^3 4l\} + e^-(kl'') \end{aligned} \tag{3.3}$$

where the initial $n = 3, 4$ complex is built by adding a $3l$ or a $4l$ electron to the target complex $\{3l^4, 3l^3 4l\}$. Similarly the DPI and PAI channels considered for the other initial complexes (up to $nl' = 10g$) were

$$\{3l^4, 3l^3 4l\}nl' + h\nu \rightarrow \{3l^4, 3l^3 4l\} + e^-(kl''') \tag{3.4}$$

$$\begin{aligned} \{3l^4, 3l^3 4l\}nl' + h\nu &\rightarrow \{3l^4, 3l^3 4l\}n'l''(n' > n, l'' \leq 5) \\ &\rightarrow \{3l^4, 3l^3 4l\} + e^-(kl'''). \end{aligned} \tag{3.5}$$

The scaling parameters of the Rydberg (other than the target orbitals) and continuum orbitals have been fixed to 1.23. This value has been obtained optimizing the scaling parameter of the Rydberg orbital 69s by minimizing all the 588 terms of the $\{3l^4, 3l^3 4l\}69s$ complex where the other orbitals were fixed to their target values.

A second IPIRDW calculation has been carried out to obtain the photoionization cross section of the Ni^{13+} ground state using the orbitals optimized in the initial atomic system of the photoionization process. This was done in order to test the influence on the cross sections of the choice of atomic orbitals. The scaling parameters of the closed shells (1s to 2p) have been fixed to 1 and those of the $n = 3, 4$ orbitals have been optimized minimizing all the 4964 terms of the Ni^{13+} complex $\{3l^4, 3l^3 4l\}\{3l, 4l\}$ ($\lambda_{1s\ to\ 2p} = 1.00, \lambda_{3s} = 1.26, \lambda_{3p} = 1.18, \lambda_{3d} = 1.18, \lambda_{4s} = 1.23, \lambda_{4p} = 1.16, \lambda_{4d} = 1.15, \lambda_{4f} = 1.27$). The scaling parameters of the other orbitals (Rydberg and continuum) have been fixed to 1.25. The latter

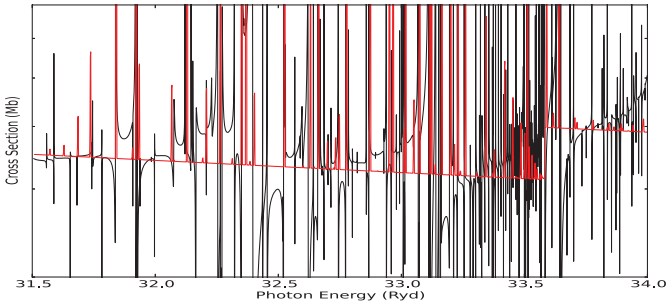

Fig. 2. Details of the total photoionization cross section for the ground state: comparison between R-matrix (in black) and our first IPIRDW calculation (in red).

has been obtained in a similar procedure as used in the first IPIRDW calculation but fixing the $n = 3, 4$ orbitals to those of the initial atomic system. The DPI and PAI channels considered were identical to those shown in Equations (3.2), (3.3).

4 Results and discussion

The cross section for the ground state of Ni XIV from our R-matrix calculation are plotted (in black) along with the results of the first IPIRDW calculation (in red) in Figure 2. We can remark the importance of the interference phenomena, while the lines added to the continuum in the IPIRDW results are all above the continuum with a symetric shape (we used a Lorentzian profile for the resonances), the structure in the R-matrix results are more complex. The interaction between the DPI and PAI channels translate into a specific asymetric Beutler-Fano profile. Hence the black plot shows features going below the continuum which correspond to a reduction of the absorption coefficient at these specific frequencies and a "large" wing above the continuum redward to the center of the line.

Differences between our first (black) and second IPIRDW (red) cross sections can be seen in Figure 3. The DPI (continuum) part of our second IPIRDW calculation that uses the orbitals optimized in the initial $(N+1)$-system is systematically overestimated with respect to our first IPIRDW model. Even the positions of the resonances and the thresholds differ significantly. Our first IPIRDW model is clearly the best choice in regard to the good agreement with our R-matrix model (see Fig. 2).

Several steps are required to calculate opacities. The first one is the determination of ionic fractions and level populations for each atom present in the plasmas. It depends on the physical conditions (T, ρ). Then given the populations one can sum the bound-bound, bound-free, free-free and scattering to obtain the opacities. We do not have all the data here to provide the full results but as an exercice we consider a plasma with only one ion, Ni xiv, populated only on the ground state. We can then quantify the effect of the interference in the opacities.

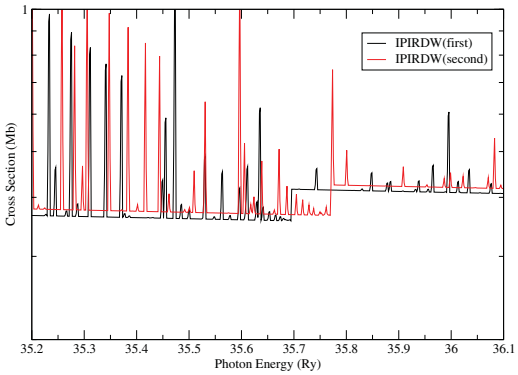

Fig. 3. Total photoionization cross section for the ground state: comparison between our first (in black) and our second IPIRDW calculation (in red).

Table 1. % difference, $\Delta\tilde{\kappa} = (\tilde{\kappa} - \tilde{\kappa}(R-\text{matrix}))/\tilde{\kappa}(R-\text{matrix})$, in the Rosseland and Planck estimate with respect to ref (high res. R-Matrix).

Methods	$\Delta\tilde{\kappa}_P$	$\Delta\tilde{\kappa}_R$
IPIRDW(first)	-0.6%	-9.6%
IPIRDW(second)	11.3%	-23.4%
R-matrix (low resolution)	-6.5%	-14.2%

For the spectral opacities we simply have the same signature as in the photoionization cross sections. It is then interesting to evaluate some mean opacities to see the effect of the Fano profiles. It is only a toy model since the temperature variation along with the density change would modify the ionic fraction as well as the populations. In the present case it is only supposed to give a first estimate on the specifics of the atomic codes. In the present case, we first omitted the weighting function in the integrand of the Rosseland and Planck mean opacity calculation. We used the following formulae for the Rosseland (κ_R) and Planck (κ_P) mean approximation respectively.

$$\frac{1}{\tilde{\kappa}_R^{bf}} = \int_0^{\nu_{max}} \frac{1}{\kappa_{bf}}(\nu)d\nu \quad and \quad \tilde{\kappa}_P^{bf} = \int_0^{\nu_{max}} \kappa_{bf}(\nu)\, d\nu.$$

In Table 1, the relative differences between "Rosseland" and "Planck" mean opacities with respect to values computed using our R-matrix model are reported for our two different IPIRDW cross sections and for our R-matrix cross section where the photon energy resolution has been degraded (R-matrix (low resolution)). One can see that the Rosseland mean is more sensitive to details of the cross sections than the Planck mean and that mean opacities based on our first IPIRDW model better agree with those based on our accurate R-matrix model even with respect

to the ones based on a low-resolution R-matrix model. The differences are of the order of the usually expected accuracies of the photoionization cross sections ($\sim$20%).

5 Conclusion and perspectives

Our preliminary results on the photoionization of Ni^{13+} ground state shows the impact of the different methods on the cross section as well as some estimated mean opacities. These differences are important given the required accuracy for application. However it is too early to draw definitive conclusion since other aspect of the calculation of opacities have not yet been included (equation of state for the population and ionic fractions, plamas conditions, etc.). Some cancellation effects can occur. The full calculation is underway, including fine structure and other ions to provide a full picture of the Ni opacities.

References

Asplund, M., Grevesse, N., Sauval, A.J., Allende Prieto, C., & Kiselman, D., 2004, A&A, 417, 751

Badnell, N.R., 2011, Comput. Phys. Comm., 182, 1528

Badnell, N.R., Bautista, M.A., Butler, K., *et al.*, 2005, MNRAS, 360, 458

Badnell, N.R., & Seaton, M.J., 2003, J. Phys. B, Atom. Mol. Phys., 36, 4367

Bailey, J.E., Rochau, G.A., Iglesias, C.A., *et al.*, 2007, Phys. Rev. Lett., 99, 265002

Bailey, J.E., Rochau, G.A., Mancini, R.C., *et al.*, 2009, Phys. Plasmas, 16, 058101

Berrington, K.A., Eissner, W.B., & Norrington, P.H., 1995, Comput. Phys. Comm., 92, 290

Blancard, C., Cossé, P., & Faussurier, G., 2012, ApJ, 745, 10

Delahaye, F., & Pinsonneault, M., 2005, ApJ, 625, 563

Delahaye, F., & Pinsonneault, M.H., 2006, ApJ, 649, 529

Delahaye, F., Pinsonneault, M.H., Pinsonneault, L., & Zeippen, C.J., 2010 [arXiv:1005.0423]

Eissner, W., Jones, M., & Nussbaumer, H. 1974, Comput. Phys. Commu., 8, 270

Fano, H., 1961, Phys. Rev. A, 124, 1866

Fu, J., Gorczyca, T.W., Nikolic, D., *et al.*, 2008, Phys. Rev. A, 77, 032713

Fuhr, J.R., Martin, G.A., & Wiese, W.L., 1988, J. Phys. Chem. Ref. Data, 17

Gilles, D., Turck-Chièze, S., Loisel, G., *et al.*, 2011, High Energy Density Physics, 7, 312

Hummer, D.G., Berrington, K.A., Eissner, W., *et al.* 1993, A&A, 279, 298

Kramida, A., Ralchenko, Y., Reader, J., & Team, N.A., 2013, NIST Atomic Spectra Database (ver. 5.1), [Online]. Available http://physics.nist.gov/asd [2013, September 19]. National Institute of Standards and Technology, Gaithersburg, MD

Montalban, J., & Miglio, A., 2008, Comm. Asteroseismol., 157, 160

Nahar, S.N., Pradhan, A. K., Chen, G.-X., & Eissner, W., 2011, Phys. Rev. A, 83, 053417

Neuforge-Verheecke, C., Guzik, J.A., Keady, J.J., *et al.*, 2001, ApJ, 561, 450

Nussbaumer, H., & Storey, P.J., 1978, A&A, 64, 139

Pinsonneault, M.H., & Delahaye, F., 2009, ApJ, 704, 1174

Richard, O., Michaud, G., & Richer, J., 2001, ApJ, 558, 377

Rogers, F.J., & Iglesias, C.A., 1992, ApJ, 401, 361

Shirai, T., Sugar, J., Musgrove, A., & Wiese, W.L., 2000, Spectral Data for Highly Ionized Atoms, Ti, V, Cr, Mn, Fe, Co, Ni, Cu, Kr, and Mo

Turck-Chièze, S., Loisel, G., Gilles, *et al.*, 2012, ed. H. Shibahashi, M. Takata & A.E. Lynas-Gray, Progress in Solar-Stellar Physics with Helio- and Asteroseismology, 462 Astron. Soc. Pac. Conf. Ser., 95